Electrochemistry in Near-Critical and Supercritical Fluids. 2. Water. Experimental Techniques and the Copper(II) System

Alex C. McDonald, Fu-Ren F. Fan, and Allen J. Bard*

Department of Chemistry, The University of Texas at Austin, Austin, Texas 78712 (Received: May 13, 1985; In Final Form: August 12, 1985)

An electrochemical cell and electrode system for investigation of aqueous systems under near- and supercritical conditions is described. Cyclic voltammetry of 1.5% w/w KCl and 6% w/w KBr solutions was investigated and log current vs. potential (Tafel) plots for the chlorine and hydrogen evolution reactions are given. A study of the Cu/Cu(I)/Cu(II) system in Na_2SO_4 and KCl solutions is described and the variation of the standard potentials of the half-reactions with temperature (to ca. 300 °C) is given. The diffusion coefficient for Cu(II) was determined by chronoamperometry as a function of temperature (22–245 °C) and shown to increase from 5.4×10^{-6} cm^2/s at 22 °C to 3×10^{-4} cm^2/s at 245 °C. The change of diffusion coefficient with temperature was larger than that predicted by the Stokes–Einstein equation at temperatures above 175 °C.

Introduction

Aqueous electrolyte solutions undergo changes in their fundamental properties and structure at elevated temperatures and pressures (greater than 100 °C and 1 bar). Over a wide range of pressure/volume/temperature (*PVT*) of near- and supercritical conditions, the physical and chemical properties of water changes through a continuum of gaslike and liquidlike forms. Above the critical point, operationally defined as the temperature (T_c = 374 °C) and pressure (P_c = 221 bar) above which the fluid is a single-phase system, small changes in the pressure and temperature can result in dramatic changes in the solvating characteristics of the medium. Aqueous solutions, in particular, undergo large changes in dielectric constant, density, and viscosity with *PVT* variations because of the transition of water from a highly associated, polar, hydrogen-bonded liquid at ambient conditions to a more disordered state at near- and supercritical conditions.

For electrochemical studies, the changes in the dielectric constant, viscosity, and density with pressure and temperature are particularly significant (Figure 1). The decrease in the dielectric constant at high temperature can be attributed to a decrease in the density and degree of association. The result is that the solvent atmosphere experienced by a solvated species become similar to that experienced in an aprotic solvent with a lower dielectric constant.[1–6] Under these conditions water becomes a good solvent for organic compounds; for example, benzene and ethane become miscible with water under supercritical conditions. This might allow studies of electrode reactions of organic species in aqueous media which are not soluble at lower temperatures. Large changes in the nature of ionic solvation can also be expected under near- and supercritical conditions. For example, changes in ion solvation have been studied for the Cu^{2+}/SO_4^{2-} system by Cobble and Murray.[7] Application of a simple Born model and calorimetric experiments showed that very strong solvent/ion interactions exist at temperatures greater than 300 °C. Although the free energy of solvation remains approximately constant, the enthalpy of hydration becomes increasingly exothermic and large heats of

solution and reaction for ions can be anticipated.

The decrease in the viscosity and density that occurs in aqueous solutions at high temperatures results in larger diffusion coefficients for solvated species. Ionic conductivities rise with temperature because of decreased solution viscosity and increased ion mobility; however, above about 300 °C, with densities below 0.6 g cm^{-3}, the conductivity decreases because of the decrease in the dielectric constant and increased ion association.[1–4,8,9] A large range of near-critical and supercritical conditions exist, however, where water shows a dielectric constant greater than 5 and aqueous solutions exhibit good conductivities.

Most previous electrochemical studies have been concerned with the variation of physical properties such as the dielectric constant and conductivity with *PVT* changes for pure water and some binary and ternary systems. In this manner, information about interionic and intermolecular interactions and kinetic phenomena has been obtained. The unique properties of near-critical water have been exploited in several separations and other applications.[10,11] However, very few studies of electrode reactions have been carried out under these conditions, probably because of experimental and apparatus design difficulties. The fundamental changes in the solvent structure around ions and at electrode surfaces suggest that electrochemical techniques may be useful probes for such systems.[12–17] Thermodynamic changes of reactions which accompany the *PVT* variations can also be investigated by measurements of electrode potentials, and new electrode reactions can be studied.

Some studies of electrode reactions in aqueous solutions at high temperatures have appeared; these mostly concern studies of corrosion[22,23] or the electrolytic decomposition of water. Most

(1) (a) Franck, E. U. *High-Pressure Chem., Proc. Nato Adv. Study Inst., 1977* **1978.** (b) Franck, E. U. "Phase Equilibrium and Fluid Properties in Chemical Industry"; Storvick, T. S., Ed.; American Chemical Society: Washington, DC, 1977; p 99. (c) Franck, E. U. *Int. Corros. Conf. Ser.* **1976,** *NACE-4,* 109.
(2) Franck, E. U.; Uematsu, M. *J. Phys. Chem. Ref. Data* **1980,** *9,* 1291.
(3) Marshall, W. L.; Franck, E. U. *J. Phys. Chem. Ref. Data* **1981,** *10,* 295.
(4) Todheide, K. "Water: A Comprehensive Treatise"; Frank, F., Ed.; Plenum Press: New York, 1972; Vol. 1.
(5) Pitzer, K. S. *Proc. Natl. Acad. Sci. U.S.A.* **1983,** *80,* 4575.
(6) Franck, E. U. *Proc. Int. Conf. High Pressure, 4th, Kyoto, 1974,* **1975,** 26.
(7) Cobble, J. W.; Murray, Jr., R. C. *Faraday Discuss. Chem. Soc.* **1978,** 144.

(8) Osusgi, J.; Shimiyu, K.; Nakahara, M.; Hirayama, E.; Matsubara, Y.; Ueno, M. *Proc. Int. Conf. High Pressure, 4th, Kyoto, 1974* **1975,** 610.
(9) Marshall, W. L. *Int. Corros. Conf. Ser.* **1976,** *NACE-4,* 117.
(10) Model, M.; Reid, R. C.; Amin, S. I. U. S. Patent 4 113 446, 1978.
(11) Gangoli, N.; Thodes, G. *Ind. Eng. Chem. Prod. Res. Div.* **1977,** *16,* 208.
(12) Neuman, Jr., R. C. *J. Org. Chem.* **1972,** *37,* 495.
(13) Sato, M.; Nakayama, E. *Proc. Int. Conf. High Pressure, 4th Kyoto, 1974* **1975.**
(14) Hills, G.; Hsieh, S. *Chem. Ing. Tech.* **1972,** *44,* 216.
(15) Hsieh, S. Ph.D. Thesis, University of Southampton, 1969.
(16) Hills, G. J. *Talanta* **1965,** *12,* 1317.
(17) Heusler, K. E. *Int. Corros. Conf. Ser.* **1976,** *NACE-4,* 387.
(18) Conway, B. E.; Currie, J. C. *J. Electrochem. Soc.* **1978,** *125,* 252.
(19) Hills, G. J.; Ovenden, P. J. *Adv. Electrochem. Electrochem. Eng.* **1966,** *4,* 185.
(20) Miles, M. H.; Kissel, G.; Lu, P. W. T.; Srinivasan, S. *J. Electrochem. Soc.* **1976,** *123,* 332.
(21) Chauvin, G.; Coriou, H.; Hardy, S. *Int. Corros. Conf. Ser.* **1976,** *NACE-4,* 293.
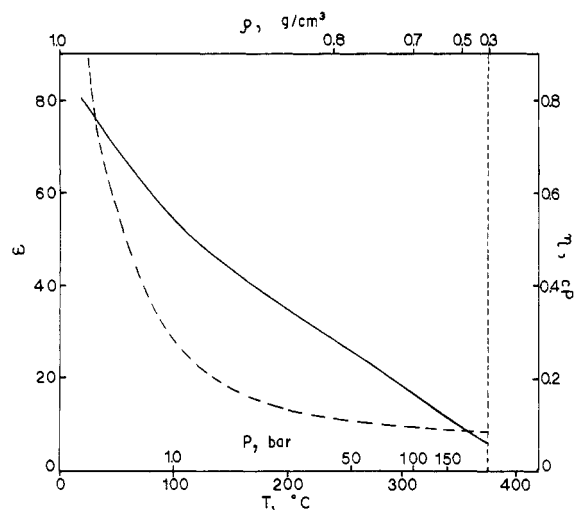(22) Berry, W. E. *Int. Corros. Conf. Ser.* **1976,** *NACE-4,* 48.

Figure 1. Dielectric constant, ϵ, (solid line) and viscosity, η, (dotted line) vs. temperature, T, pressure, P, and density, ρ, for a two-phase system of pure H_2O.[1,27,34] Critical point shown $T_c = 374\ °C$, $P_c = 221$ bar, $\rho_c \cong 0.32$ g cm^{-3}, $\eta_c \cong 0.098$ cP, and $\epsilon \cong 5.8$.

of the work on the anodic evolution of oxygen and cathodic evolution of hydrogen at elevated temperatures and pressures has examined the processes under subcritical conditions to elucidate the kinetics of the reactions.[16-21] At high temperature, the polarizable range of metal and metal oxide electrodes decreases because of a decrease in the overpotentials and the thermodynamic shifts in the standard potentials for the oxygen and hydrogen evolution processes. For example, at nickel oxide electrodes in alkaline solutions, the potential window was observed to decrease to approximately 1.0 V [i.e., between 0.0 and +1.0 V vs. a dynamic hydrogen electrode (DHW)] by 264 °C.[20] Under supercritical conditions, the polarizable range of iron electrodes in aqueous solution was reported to be reduced to essentially zero by 400 °C.[2] This observation probably represents the corrosion and electrodissolution of the anodic material, since $\Delta G°$ for the water decomposition reaction does not become zero until much higher temperatures (ca. 4000 °C).

The characterization of the effect of temperature and pressure on the rate and pathway of an electrode reaction is more difficult. Higher temperatures, as described above, are generally accompanied by increased ionic conduction and diffusion rates due to a decrease in viscosity. The effect of pressure is more complicated, and increased pressure can result in a decrease in the rates of diffusion and changes in the degree of ionization of electrolytes. It is the combined changes in pressure and temperature, particularly in aqueous systems, which result in the fundamental changes in the solvent (dielectric constant, degree of association, enthalpy of solvation) which produce the unique properties of these systems. For example, the pressure dependence of various electrode process parameters at low temperatures has been studied, but the changes are small; a pressure variation of several kilobars is necessary to cause significant changes in reaction rates at 25 °C. Thus, studies at high pressures at ambient temperatures are not relevant to processes under near- and supercritical conditions, where relatively small pressures are required for fluid containment. A complete study of a simple electrode process under near-critical conditions has yet to be reported.

Problems exist in choosing a well-behaved test system to investigate the use of electrochemical techniques as probes in near- and supercritical aqueous solutions. The decreased potential window available at elevated temperature restricts the number of electroactive species which can be examined. Moreover, because the standard potentials of redox processes shift relative to the solvent limits, it is difficult to predict the accessibility of a given system. Lack of thermodynamic data under these conditions has also made choice of suitable redox systems more difficult.
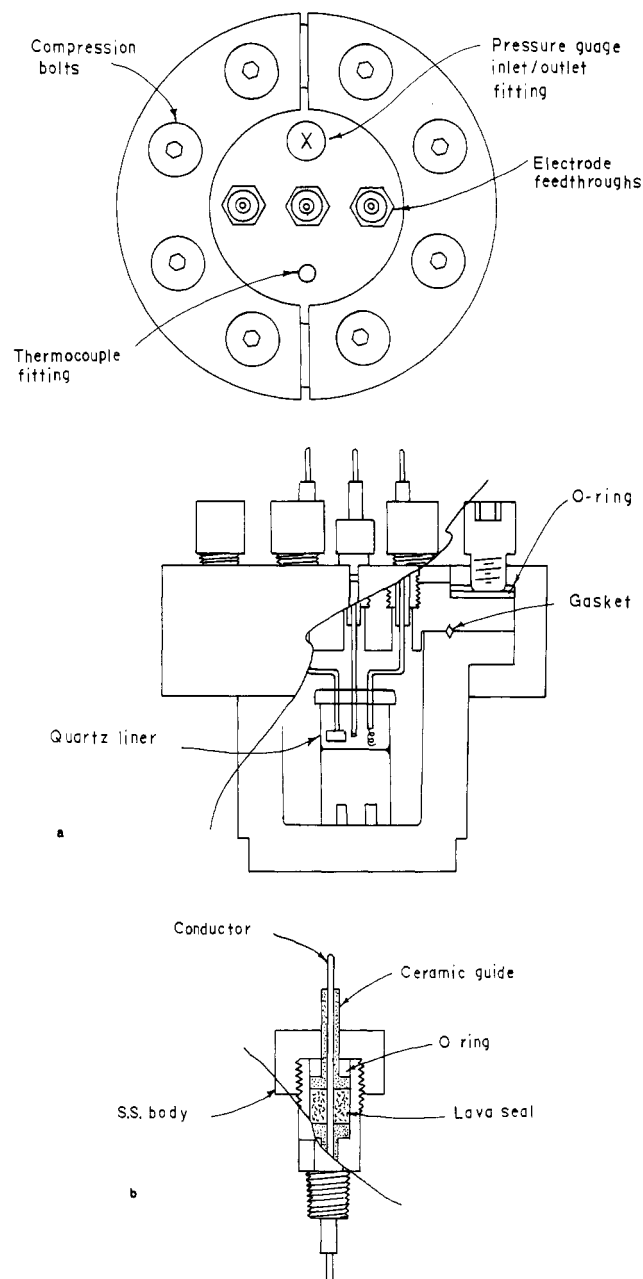
(23) Vermilyea, D. A.; Indig, M. E. *J. Electrochem. Soc.* **1972**, *119*, 39.

Figure 2. (a) Schematic diagram of autoclave and gauge block assembly. All components are 316 stainless steel unless indicated. (b) Electrode feedthrough assembly.

A serious problem to be addressed in these studies is the corrosion of the cell materials and the alteration of the electrode surface by high-temperature fluids. The solution must be contained in a suitable vessel and electrodes of the proper configuration must be inserted with feedthroughs through the vessel's walls. No contamination of the solution by corrosion products should occur during the experiment. Extensive work has been reported on the rates of corrosion of various metals and alloys in aqueous solutions at elevated T and P.[22,23] Most of this work has addressed the corrosion of structural materials for industrial applications. The presence of corrosion products at concentrations which can be tolerated in these environments generally precludes the use of most metals for electroanalytical cells.

In this paper we describe experimental apparatus and methodology for studies of near- and supercritical aqueous solutions. Examination of the accessible potential range in alkali metal halide electrolyte solutions under critical and near-critical conditions and the use of electrochemical techniques as probes in these systems is demonstrated. The $Cu/Cu(I)/Cu(II)$ system in Cl^- and $SO_4{}^{2-}$ media was characterized from room temperature to near-critical conditions by voltammetric techniques and relative potentials and

diffusion coefficients are reported.

Experimental Section

The containment pressure vessel used in these experiments was a Parr Instruments (Parr Instrument Co., Moline, IL) Model 4651 autoclave made entirely from 316 stainless steel (see Figure 2a). The head assembly of the pressure vessel was drilled and tapped to accept a Parr Instruments Model 4317 pressure gauge and a valve, a sheathed Type J thermocouple, and three electrode feedthroughs. The head assembly was mated and sealed to the body with a nickel–chrome compression gasket. All external threaded surfaces were lubricated with a silver-based high-pressure lubricant (Silver Goop; Crawford Fitting Co., Solon, OH) to inhibit corrosion and seizing. A closed, but not sealed, quartz linear was used as the electrochemical cell to contain the fluid under subcritical conditions. Although silica is slightly soluble in high-temperature aqueous solutions,[24] the extent of attack of the quartz and solution contamination during a typical experimental run (6 h) was not considered to be a significant factor with the systems studied. This cell configuration was chosen to minimize the contamination of the working solution by cell corrosion products from the outer pressure vessel and electrode feedthroughs. In addition, the interior surfaces of the pressure vessel were polished periodically to discourage pit and crevice corrosion. Satisfactory behavior was obtained for neutral alkali metal halide solutions provided the solution and vessel were deoxygenated. This was achieved by purging the solution and vessel interior with high-purity nitrogen prior to vessel closure, heating, and pressurizing. The resulting solvent is therefore a binary mixture of H_2O-N_2. Water–inert gas mixtures known to have a high degree of miscibility at high temperatures and pressures and have continuous critical curves for the conditions studied in this work. Previous studies have indicated that H_2O-N_2 mixtures exhibit increased P_c values as the mole fraction of N_2 was increased, but only slight deviations in T_c.[4,33] The P vs. T relation of the mixtures studied did not deviate from those of pure water within the limits of uncertainty of the experimental measurements. Reduction of N_2 is thermodynamically and kinetically possible at potentials near those for hydrogen evolution in the cell, since the temperature and pressure conditions approach those of the Haber process. While the N_2 reduction process was not examined in the studies reported here, the presence of N_2 probably did not affect the electrochemical results, since the rate of this reaction is quite low at these temperatures. The presence of even minute quantities of oxygen promoted corrosion of the stainless steel cell components and caused the precipitation of metal (Fe, Cr, and Ni) oxides from solution. Irreproducible electrode surface conditions were also observed when oxygen was present in the system. For this reason, evolution of oxygen at the working electrode was generally avoided. For each set of experimental measurements in which the pressure vessel and cell were loaded, heated, and pressurized, the working solution was evaluated for contamination with metal ions by in situ observation of the current–voltage characteristics at a Pt electrode and, after cooling, by spot tests and polarographic analysis of the solution.

The electrode feedthrough assemblies presented unique problems because conventional high-pressure sealing materials (e.g., Teflon, epoxy) are not suitable for high-temperature applications.[15,24] The feedthrough which was found to provide a gas-tight seal under these conditions, was a Conax Model EG-093 (Conax Corporation, Buffalo, NY) with 2-mm-diameter conductors and fully supported grade A lava seals (see Figure 2b). Two different working electrode designs were used. For low- and medium-temperature applications (less than 250 °C), a Pt disk, sealed in cobalt glass and welded to a 2-mm stainless steel conductor passing through the electrode feedthrough, was employed. The conducting rod was masked with Teflon to prevent contact with the working solution. This Teflon mask was leakproof for several temperature cycles. The electrode surface was prepared by mechanical pol-

ishing with 3-μm diamond grit paste followed by ultrasonic cleaning in methanol. The counter electrode of a similar configuration was a Pt flag of area of about 0.5 cm².

At temperatures greater than 250 °C, the above electrode configuration was not suitable because of leakage around the Teflon seal. To overcome this problem, the stainless steel electrode feedthrough conductors were replaced with tantalum rods of the same dimensions. Pt foil was arc welded directly to the butt end of the Ta rod and its surface prepared and polished as described above. The entire electrode assembly was then anodically polarized in 0.1 M HNO_3 until the Ta surface was passivated by an oxide layer. Thus, a known area of Pt electrode was provided. The same procedure was used for the counter electrode, with a Pt flag of area of about 0.5 cm². This electrode configuration was stable during repeated cycling (greater than 25 times up to 400 °C at 340 bar). No dissolution of the passivating oxide layer on the Ta conducting rods was observed and care was taken not to polarize the electrode to the cathodic limit under high-temperature conditions to prevent the possible reduction of the oxide. The resistance between the leads in an empty cell was greater than 200 MΩ at ambient conditions and remained greater than 1 MΩ at 400 °C.

The choice of a reference electrode proved difficult and several were employed with moderate success. In some solutions containing a chloride electrolyte salt, an Ag wire coated with AgCl immersed directly in the working solution was used. The temperature and pressure dependence of the electrode potential of the Ag/AlCl electrode with respect to a hydrogen electrode has been reported up to about 250 °C.[26] For the characterization of supporting electrolytes in the absence of an added redox couple, a tungsten wire coated with an anodically formed oxide was used. The tungsten wire was welded directly to the tantalum rod and was inserted into the working solution. Although the temperature and pressure dependence of this quasi-reference electrode is not known, it proved to be stable for a given set of PVT conditions. Some temporary fluctuations in the potential did occur when large amounts of bromine were generated at an electrode in the vicinity of this reference electrode. The tungsten wire reference electrode could not be used in solutions containing Cu(II). At temperatures greater than 200 °C, rapid variations in the potential occurred and Cu^0 was observed to coat the tungsten wire, probably because of the direct reduction of Cu(II) to Cu with the oxidation of tungsten to tungsten oxide. For the experiments performed with Cu(II) in solution, a copper reference electrode was employed. High-purity copper foil was welded onto the tantalum rod and inserted into a separate quartz compartment which contained a small amount of the Cu(II) test solution. The reference compartment was connected to the working compartment with an asbestos wick saturated with 0.2 M Na_2SO_4. No contamination of the working solution with Cu^{2+} ions through the wick was observed during the experiments. With these reference electrodes, potentials could not be referenced to the NHE, but the relative potentials and potential shifts of electrochemical processes were characterized.

The entire pressure vessel was heated in a stainless steel sheathed oven and the temperature controlled within ±3 °C by a Parr Instruments Model 4821 controller. From the solution temperature and pressure, the solution properties (e.g., volume, density) relative to the critical point could be approximated. To allow for the pressurization of the vessel with increased temperature without a large amount of vaporization of the working solution, 50 cm of distilled water was placed in the vessel outside the quartz liner. Between 12 and 15 cm³ of the working solution was then placed within the liner. The initial volume of solution was chosen to provide the desired solution density and total volume at elevated temperature. The solution volume at subcritical temperatures and pressures was estimated from thermodynamic data for pure H_2O.[27] The system was allowed to equilibrate for approximately 1 h after

(24) Downs, J. L.; Payne, R. T. *Rev. Sci. Instrum.* **1976**, *40*, 1278.
(25) Wilde, B. E. *Int. Corros. Conf. Ser.* **1976**, *NACE-4*, 277.

(26) Macdonald, O. D. *J. Electrochem. Soc.* **1979**, *126*, 908.
(27) "Handbook of Chemistry and Physics", 51st ed.; Weast, R. C., Ed. CRC Press: Boca Raton, FL, 1970.
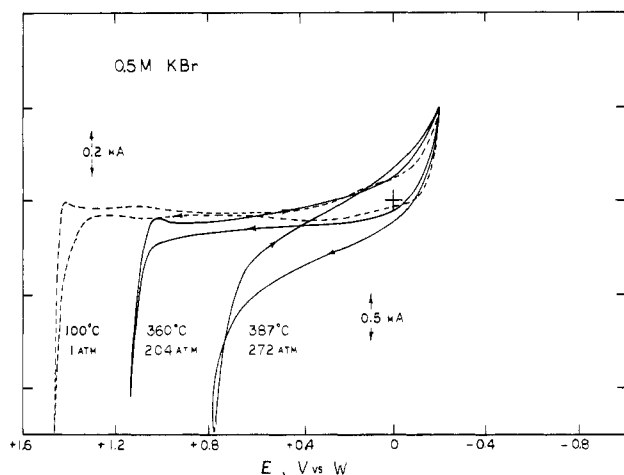
Figure 3. Current–potential curves of a Pt electrode in KBr (0.5 M at 25 °C) at several temperatures and pressures. Scan rate = 100 mV s^{-1}.
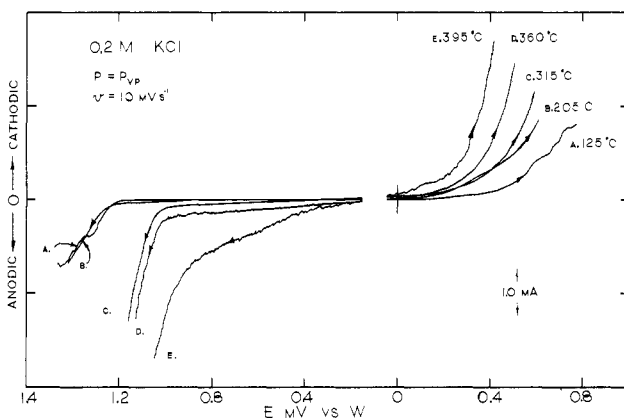

Figure 4. Current–potential curves of a Pt electrode in KCl (0.2 M at 22 °C) at several temperatures and pressures. Scan rate = 10 mV s^{-1}.

heating to the desired temperature to minimize thermal gradients and convection. It was not possible to eliminate convection completely because of some uneven heating of the vessel.

All solutions were prepared from triply distilled water. The KCl, KBr, and CuCl$_2$ salts were recrystallized from triply distilled water and dried prior to use. All the remaining compounds were reagent grade and were used without further purification. Conventional electrochemical instrumentation (potentiostat, function generator) was employed.

Results and Discussion

KCl and KBr Solutions. Initial studies of the supporting electrolyte solutions at a Pt electrode were carried out to observe the background processes (hydrogen and halogen evolution) and ascertain the useful potential range for the investigation of other processes. The polarizable limits of a Pt electrode with these supporting electrolytes decreased with an increase in temperature and pressure. Current–potential (*i–E*) curves obtained by cyclic voltammetry at a Pt electrode in KBr and KCl solutions are shown in Figure 3 and 4. The potential scale is given vs. the reference electrode potential at the temperature and pressure of the solution under investigation. The magnitude of the decrease in the polarizable range is generally similar to that reported previously for subcritical conditions.[20] The precise values of T_c and P_c for these solutions were not measured; however, critical curves published for NaCl–H$_2$O systems indicate that a 1.5% (by weight) solution of KCl–H$_2$O at 395 °C at 289 bar is supercritical. Critical curves are not available for the KBr–H$_2$O systems, but they probably are similar in manner to the KCl–H$_2$O solutions so that the data for the 6% (by weight) solution of KBr at 387 °C at 272 bar are very near to critical conditions. Both of these solutions are above the critical point of pure water and have densities of approximately 0.36 ± 0.03 g cm^{-3}. No distinct transition in the electrochemical

behavior was observed as the solutions approached and exceeded the critical point. It has been reported previously that alkali metal halide/water solutions remain homogeneous, even above the critical point of pure water and at salt concentrations of 10% by weight and higher.[1,2,4] The electrochemical processes observed in these experiments demonstrate that near- and supercritical aqueous solutions have densities and ionic conductivities that are suitable for electrochemical measurements. Most significant is that, contrary to previous reports,[2] potential windows, of about 800 and 1100 mV in KBr and KCl solutions, respectively, remain at the critical point.

An increase in the temperature and pressure caused significant changes in the *i–E* characteristics in the KBr and KCl solutions in the so-called double layer region (between the limiting reduction and oxidation processes). Most notable was an increased difference of the base-line current on anodic and cathodic sweeps as well as an increase in the magnitude of the current (see Figure 3). The slope of the base line was also greater at higher temperatures. At slower sweep rates, peak broadening decreased, but the slope remained constant under these conditions. The broadening of the base line also decreased slightly when the potential was scanned repeatedly within this region to the potential limits of the solution. This behavior is probably caused by several factors. (1) The rate of diffusion of electroactive impurities increases with increasing temperature as the solution viscosity decreases. A contribution from thermal convection to mass transfer probably also contributes to the increased current. (2) Penetration of solution between the electrode feedthrough rods and the vessel body at higher T and P could result in the sloped and broadened base line, by altering the interelectronic resistance and capacitance. It is unlikely that an increase in solution resistance caused by ion association contributes, since previous studies have indicated that only a two- or three-fold decrease in the specific conductance should be experienced in these temperature ranges. (3) The formation of a surface layer on the Pt electrode may occur to produce "capacitive-like" currents from its oxidation and reduction.

The behavior observed for these systems was the same when the electrochemical experiments were first begun at high temperature and the solution cooled, as when the experiment was begun at low temperature and the solution heated. The results were also the same when positive feedback *iR* compensation was employed.

Tafel plots (ln (*i*) vs. *E*) for the limiting processes, presumably the evolution of hydrogen and chlorine at the Pt electrode in KCl solution, at several temperatures and pressures are shown in Figure 5. The potential scale has not been corrected for the temperature and pressure variation of the reference electrode potential with respect to NHE. The curvature of the ln (*i*) against potential plots for chlorine evolution has been attributed to the occurrence of the following reaction at high overpotentials[28]

$$Cl^- + Pt \rightarrow PtCl_{ads} + e \qquad (1)$$

$$2PtCl_{ads} \rightarrow 2Pt + Cl_2 \qquad (2)$$
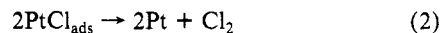
The facts that the curves have the same shape at different T and P suggests that the mechanism is the same under all conditions.

ln (*i*) vs. *E* plots for H$_2$ evolution are linear over the range of potentials examined and show an increased slope with increasing T and P (Figure 5). From the Butler–Volmer equation[29] the "effective cathodic transfer coefficient", α, for this process obtained from the slope of the ln (*i*)–E curve changes from about 0.22 at 125 °C to 0.64 at 387 °C. Similar changes of α with T have been reported for this process at temperatures up to 264 °C.[20] The significance of these changes is not apparent. It is possible that the variation in the slope of the Tafel plots with temperature can be mainly attributed to the variation of the activity of protons because of changes in the ion product of water as a function of temperature (Figure 6). Note that the Tafel slopes for H$_2$

(28) Novak, P. *J. Electrochem. Soc.* **1979**, *126*, 209.
(29) See, for example: Bard, A. J., Faulkner, L. R. "Electrochemical Methods: Fundamental and Applications"; Wiley: New York, 1980; p 143.
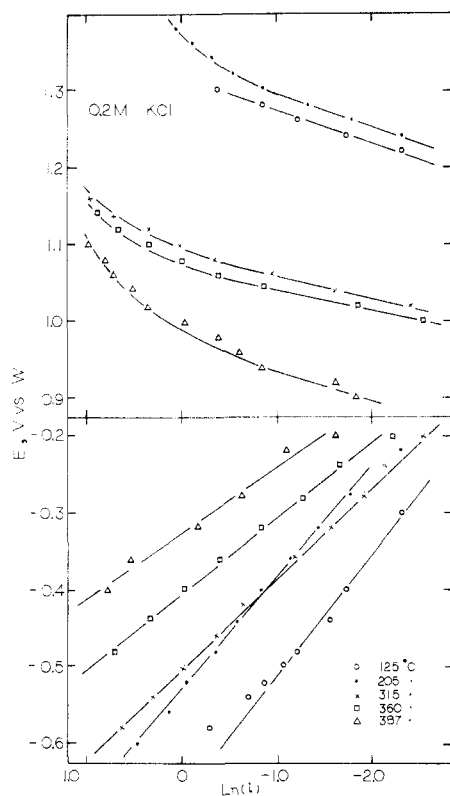
Figure 5. ln (current)–potential curves (E) 0.2 M KCl (at 22 °C) at several temperatures and pressures.
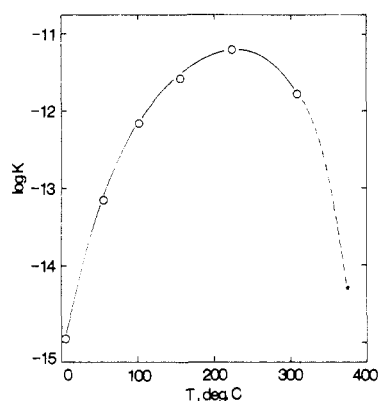

Figure 6. Ion product of pure liquid H_2O (K_w) against solution temperature for a two-phase system. Solid line drawn through the circles is experimental,[36] and the dashed line is calculated.[4]

evolution qualitatively show the same trend with increasing temperature as does the ion product of water, both reaching a maximum near 210 °C. This conclusion may be an oversimplification, since there are at least eight possible species present in the KCl solution at near-critical conditions including K^+Cl^-, K^+, Cl^-, K^+OH^-, H^+Cl^-, H^+, and OH^- and ion pair association may occur to a significant extent.[30] A change in the relative activity of H^+ and OH^- could account for the observed results; however, definite conclusions about the mechanism for H_2 evolution are not possible on this basis. Exchange current densities were not estimated because the standard potentials for the processes were not known with the reference electrode employed.

Cu^{2+} in KCl and Na_2SO_4 Solutions. A primary objective of this study was the examination of a well-defined redox reaction as the temperature was increased from ambient conditions to near the critical point to see if voltammetric techniques could be employed. Because of the small polarizable range of an electrode in aqueous solution and the increased reactivity of chemical species at high temperatures, the choice of a suitable, uncomplicated redox
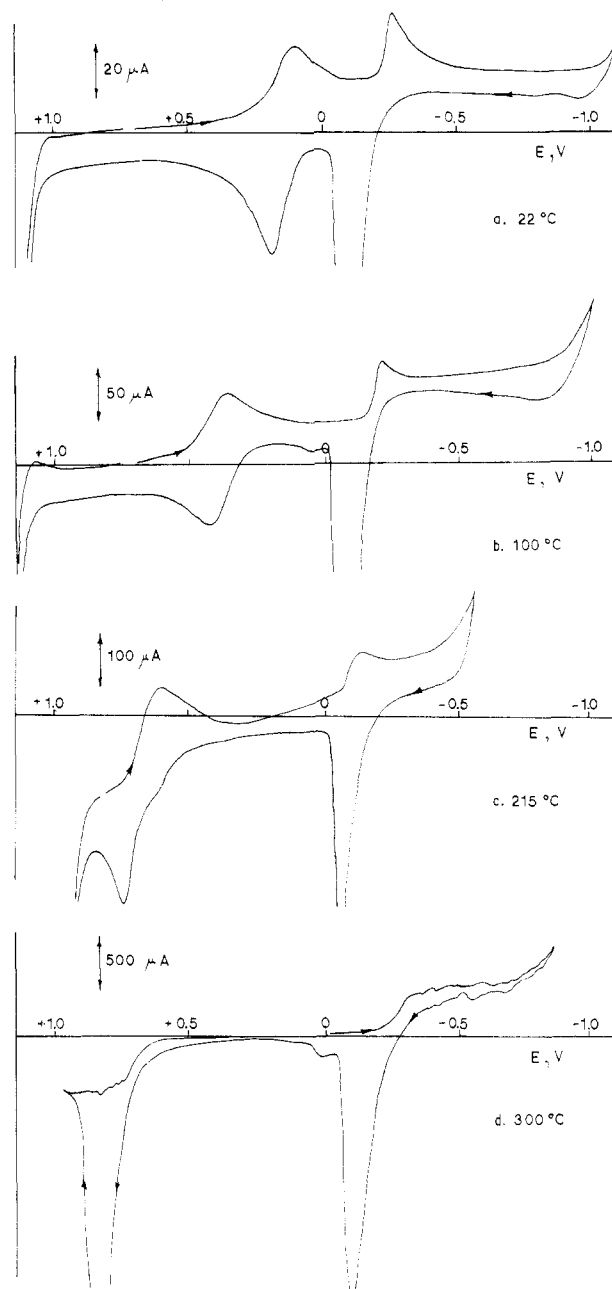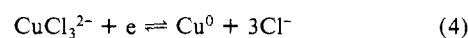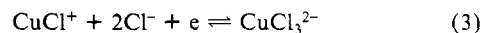
(30) Pitzer, K. S.; Li, Y. *Proc. Natl. Acad. Sci. U.S.A.* **1984**, *81*, 1268.

Figure 7. Current–potential curves recorded with 8.0 mM $CuCl_2$ in 0.2 M KCl (at 22 °C). The solution temperature and pressure are (a) 22 °C at 15 psi, (b) 100 °C at 15 psi, (c) 215 °C at 300 psi, (d) 300 °C at 1190 psi. The potential scale is vs. Cu^0/Cu^{2+} and current scale as indicated. Scan rate, 100 mV s⁻¹.

reaction which could be probed over the whole range of conditions was limited. The Cu/Cu(I)/Cu(II) system in sulfate and chloride media was found to produce relatively well-defined waves over a wide range of temperatures and pressures in rigorously deoxygenated solutions.

Current–potential curves for a Pt electrode in a KCl solution containing $CuCl_2$ at different temperatures and pressures are shown in Figure 7. No evidence of hydrolysis or precipitation of copper species was observed under these conditions over the temperature range employed. Under ambient conditions, two waves are observed. Near +0.13 V, Cu(II) (predominantly in the form of $CuCl^+$ at ambient conditions) is reduced to Cu(I) (as $CuCl_3^{2-}$). At –0.2 V, the reduction of Cu(I) to Cu metal occurs:

$$CuCl^+ + 2Cl^- + e \rightleftharpoons CuCl_3^{2-} \qquad (3)$$

$$CuCl_3^{2-} + e \rightleftharpoons Cu^0 + 3Cl^- \qquad (4)$$

These redox reactions are written for the predominant species present in 0.5 M KCl at 25 °C.[31] The potential of the Cu(II)
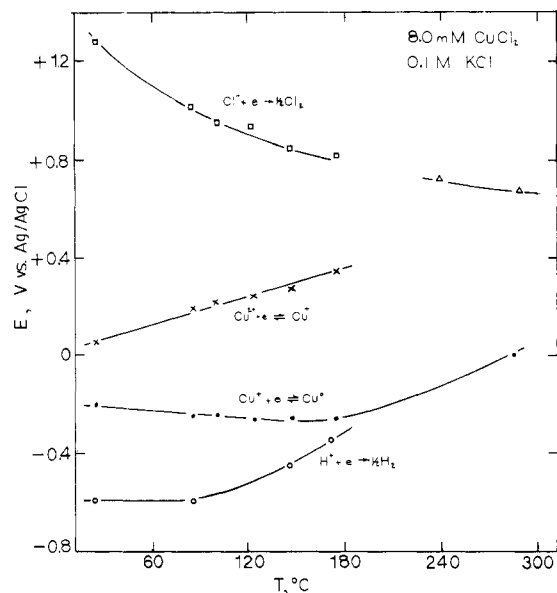
Figure 8. Potentials vs. solution temperature for various electrode processes at a Pt electrode in 0.1 M KCl containing 8.0 mM $CuCl_2$. The potentials have not been corrected for the temperature and pressure dependence of the reference electrode. The system pressure at a given temperature is equal to the vapor pressure of the solution.

Figure 9. Current, i, vs. $t^{-1/2}$ for the reduction of Cu^{2+} to Cu^0 calculated by potential step chronoamperometry at several temperatures and pressures. 8.0 mM $CuSO_4$, 0.2 M Na_2SO_4 (at 22 °C).

Figure 10. Diffusion coefficient of Cu(II), D, calculated from chronoamperometry data (solid line) and calculated from eq 6 (dotted line), vs. temperature. The system pressure at a given temperature is the vapor pressure of the solution.

reduction shifted in a positive direction (vs. a Cu/Cu(II) reference electrode) with an increase in temperature, because of a change in the relative stability and solvation of the Cu(II) and Cu(I) species with the change in solution characteristics (Figure 7). This shift of the standard potential of the Cu(II)/Cu(I) reaction is indicative of a stabilization of the cuprous species relative to the cupric species. The relative shifts in the potential of the different half-reactions as a function of solution temperature are summarized in Figure 8. At temperatures greater than 200 °C, the potential at which the reaction in eq 3 occurred had shifted into the Cl_2 evolution wave and a separate wave could not be observed. This implies that at temperatures above 200 °C, Cu(II) will spontaneously oxidize Cl⁻ to chlorine. Similar behavior was observed for other KCl concentrations.

The potential at which Cu metal was deposited on the electrode surface varied erratically within a 200-mV range as the temperature was increased, perhaps because of irreproducible variations of the Cu^0 activity on the Pt; however, the potential of the stripping peak ($Cu^0 \rightarrow$ Cu(I)) remained constant relative to the copper reference electrode. A negative temperature coefficient for the $E°$ of this reaction in aqueous media has been reported previously.[32] The variation of the reduction wave position might also be due to changes in the electrode surface condition during the course of the experiment. Repeated formation and removal of a Pt compound surface layer on the electrode during deposition and stripping of a Cu^0 layer would contribute to different conditions for film nucleation and formation. A marked positive shift in the potential of H_2 evolution on Cu^0 with increasing temperature was observed. This was probably due to a decrease in the overpotential of the proton reduction process.[19] By about 250 °C, the potential for H_2 evolution and Cu^0 deposition are coincident.

In a solution containing Cu(II) the characteristics of the Cl⁻ oxidationwave underwent a marked change at the temperature at which the Cu(II) reduction wave and the Cl_2 evolution wave became coincident. At this point, a large anodic peak was observed in the current–potential characteristics which resulted in the apparent passivation of the electrode surface (see Figure 7, 300 °C). If the potential was reversed prior to the peak potential of this anodic trace, the reverse trace followed the forward trace. The logarithm of the peak anodic current was directly proportional to the KCl concentration and independent of the Cu(II) con-
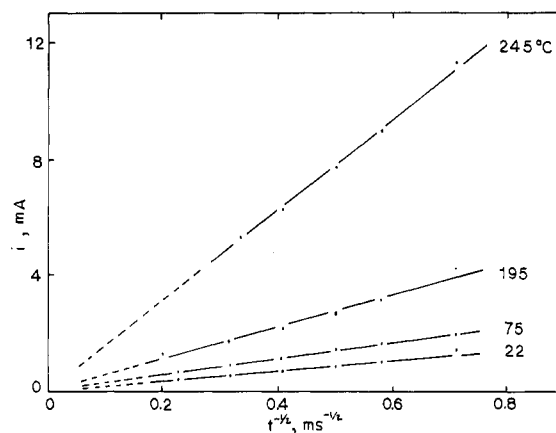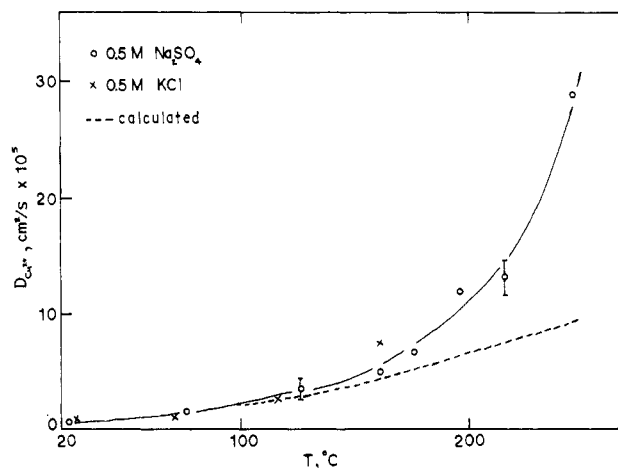
centration, although such effects were not seen in KCl solutions in the absence of Cu(II).

As the temperature increases, the onset of convection causes distortion of the cyclic voltammetric wave shapes at scan rates at or below 100 mV s⁻¹; this is particularly evident in the voltammogram at 300 °C (Figure 7). Because of contributions by thermal convection to mass transport on the time scale of the cyclic voltammetric scans, chronoamperometry at shorter times was employed to obtain values of the diffusion coefficients for the electroactive copper species as a function of temperature and pressure. For times between 20 and 100 ms for potential steps beyond the CV peak potential, the redox processes were diffusion-controlled and the Cottrell equation (eq 5) was followed.[29]

$$i(t) = nFAD^{1/2}c^*/\pi^{1/2}t^{1/2} \qquad (5)$$

Characteristic i vs. $t^{-1/2}$ plots for a cathodic potential step at different temperatures are shown in Figure 9. For times below 10 ms, the measured current contained an appreciable nonfaradaic component. At longer times (beyond about 100 ms), after the application the potential pulse, the measured current exceeded that expected from diffusion alone and eventually leveled off to a steady value. This contribution to mass transport by convection became more significant as the temperature was increased. Between these limits, a time window existed for which the process appeared diffusion-controlled and was characterized by linear vs. $t^{-1/2}$ plots with zero intercepts.

Values of the diffusion coefficient for the electroactive Cu(II) species were calculated from the slopes of the Cottrell plots. The Cu(II) concentration, C^*, was obtained from the known initial concentration and the changes in density of the solution with T

(31) Barry, T. I. *ACS Symp. Ser.* **1979**, *133*, 681.
(32) Bertocci, U.; Turner, D. L. In "Encyclopedia of Electrochemistry of the Elements"; Bard, A. J., Ed.; Dekker: New York, 1974; Vol. 2, p 384.

TABLE I: Variation of Diffusion Coefficient of Cu(II) in Na₂SO₄ with Temperature

T, °C	η,[a] cP	$D \times 10^5$,[b] cm²/s	$D_0 \times 10^5$,[c] cm²/s
22	0.955	0.54	0.57
75	0.38	1.7	1.68
125	0.22	3.6	3.31
160	0.17	4.9	4.67
175	0.152	6.31	5.40
195	0.135	11.9	6.35
215	0.120	13.0	7.45
245	0.105	29.8	9.04

[a] See ref 28, 34, and 36. [b] $D = \pi/(nFAC)^2 m$, where m is slope of i vs. $t^{-1/2}$. [c] $D = kT/6\pi\eta a$.
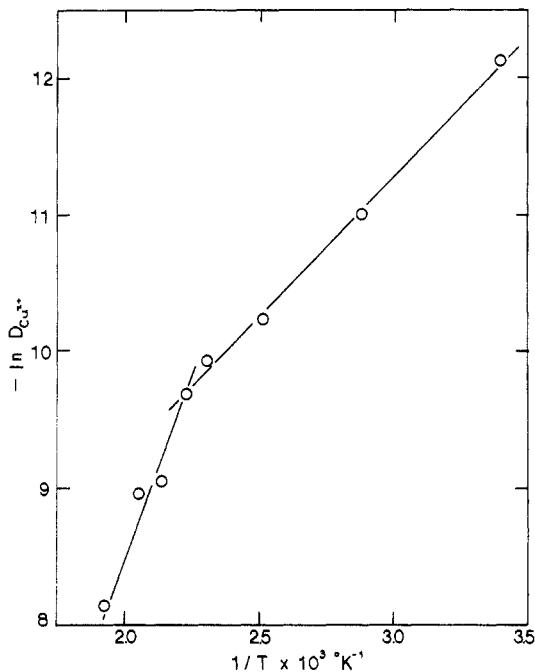
**Figure 11.** ln D vs. $1/T$ from data in Figure 10.

and P. The calculated diffusion coefficient of the Cu(II) species in a Na₂SO₄ electrolyte against temperature are shown in Table I and Figure 10. A similar trend was observed for KCl electrolytes (Figure 10). At elevated temperatures, the calculated diffusion coefficient exceeds that predicted by the Stokes–Einstein relationship:

$$D = kT/6\pi\eta a \quad (6)$$

where η is the solution viscosity and a is the diameter of the solvated ion (assumed to be spherical). This suggests that the changes in D with temperature are not solely caused by a decrease in solution viscosity. As shown in Figure 11, a plot of ln D vs. $1/T$ shows a distinctly larger slope at the higher temperatures, suggesting an increase in the energy of activation of diffusion from 17 to 45 kJ mol⁻¹. If we ascribe this change to a change in solvation and a decreased effective solvated ion diameter, a, we can calculate values of a from eq 6 (Figure 12). We might note that similar variations in a have been found in fitting conductance data and interpreting ion pair dissociation constants under supercritical conditions.[33]

Conclusions

The use of electrochemical techniques as probes in near- and supercritical aqueous solutions has been demonstrated. At temperatures and pressure up to and greater than T_c and P_c (for pure
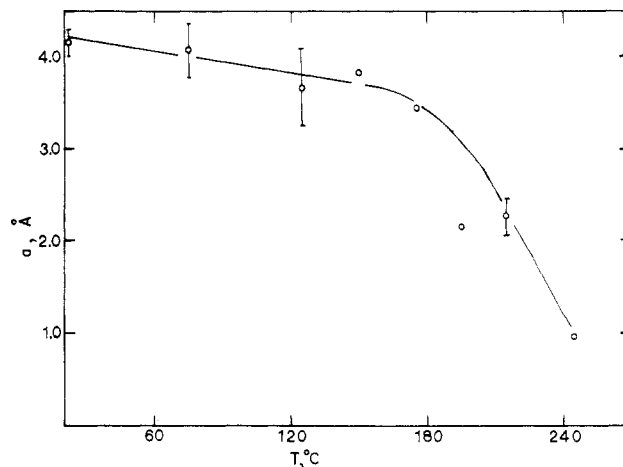
Figure 12. Plot of the effective ion diameter, a, calculated from the data in Table I and eq 6 against solution temperature.

H₂O), the density and conductance of alkali metal salt solutions remain sufficient to observe electrochemical processes. Although the polarizable range of a Pt electrode decreased with increased T and P, approximately a 1.0-V range between the background processes was observed for near-critical conditions. This suggests that suitable redox reactions can be studied under these conditions to extract thermodynamic and kinetic information.

The diffusion coefficient of Cu(II) in Cl⁻ and SO₄²⁻ media, measured by using chronoamperometry, increased dramatically with T and P and at T greater than 160 °C (up to 250 °C) exceeded that predicted from viscosity considerations alone. The potential of Cu(I)/Cu(II) redox reaction exhibited a positive temperature coefficient due to the increased stability of the Cu(I) species relative to the Cu(II) species as the solvating properties of the solution changed with T,P.

Electrochemistry in near- and supercritical water may have practical applications. Changes in the thermodynamics of reactions and improved kinetics at higher temperatures may make accessible reactions that are not possible near ambient conditions. The improved kinetics and greatly increased mass-transfer rates imply operations at higher current densities and throughputs. Moreover, the different solvent characteristics of water under near-critical conditions allow organic compounds that are insoluble in water at lower temperatures (e.g., benzene) to be dissolved and electrolyzed. The ability to change solvation characteristics and solubilities by variation of T and P also can lead to improved separations of products.

Although the cell and bomb described here have been useful in these preliminary studies, this type of system has several disadvantages. Long thermal equilibration times are required, so that examination of a single system over a range of temperatures requires a long time. The solution conditions cannot readily be changed during an experiment, and neither can the electrodes be removed and replaced for inspection and cleaning. Finally the solution tends to become contaminated with small amounts of corrosion products during the extended duration of an experiment. To overcome some of these problems, a flow system involving small diameter tubing and local heating in a small alumina tube cell has been devised.[37] Experiments with this new system are currently under way.

(33) Hartman, D.; Franck, E. U. *Ber. Bunsenges. Phys. Chem.* **1969**, *73*, 514.
(34) Dudziak, K. H.; Franck, E. U. *Ber. Bunsenges. Phys. Chem.* **1966**, *70*, 1120.
(35) Pitzer, K. S.; Li, Y. *Proc. Natl. Acad. Sci. U.S.A.* **1984**, *81*, 1268.
(36) Noyes, A. A. "The Electrical Conductivity of Aqueous Solutions"; Carnegie Institution: Washington, DC, 1907; Publ. No. 63.

(37) Flarsheim, W.; Johnson, K.; Bard, A. J., unpublished experiments.